BOUNDARY-INTEGRAL METHODS FOR ITERATIVE SOLUTION OF SCATTERING PROBLEMS WITH VARIABLE IMPEDANCE SURFACE CONDITION

F. Collino, F. Millot, and S. Pernet

CERFACS
42, Avenue Gaspard Coriolis
31057 Toulouse Cedex 01, France

Abstract—We present an efficient boundary element method to solve electromagnetic scattering problems relative to an impedance boundary condition on an obstacle of arbitrary shape in the frequency domain. In particular, the technique is based on a Combined Field Integral Equation (CFIE) and is well adapted to treat the partially coated objects. Some methods are then proposed in order to eliminate the magnetic current and to treat correctly the rotation operator $\mathbf{n} \times \cdot$ (where $\mathbf{n}$ is the unit outward normal). After discretization, the final system is solved by an iterative method coupled with the Fast Multipole Method (FMM). Finally, a numerical comparison with a well-tried method to solve this kind of problem proves that we have proposed an attractive technique in terms of memory storage and CPU time.

1. INTRODUCTION

This paper is concerned with the solution of electromagnetic scattering problems by an obstacle whose surface is covered by thin layers of imperfectly conductor materials. This type of materials is generally taken into account by imposing an impedance boundary condition like the Leontovitch condition [1] on the surface of the object. This latter connects the tangential component of the magnetic field with the tangential trace of the electric field. More precisely, the boundary condition is: $\mathbf{n} \times (\mathbf{E} \times \mathbf{n}) = Z_0 \eta (\mathbf{n} \times \mathbf{H})$ where $\mathbf{E}$ and $\mathbf{H}$ are the electric and magnetic fields respectively, $\mathbf{n}$ is the outgoing unit normal to the surface of the object, Z_0 is the intrinsic impedance of the vacuum and $\eta(x)$ is the impedance. More sophisticated models can be derived, replacing the function $\eta(x)$ by some operator acting on the

currents [22, 29]. It was recognized that this type of boundary condition can be extensively used to get a tractable problem in numerous complex situations. A first example can be found in radar applications: objects are often partially coated by a thin dielectric layer to reduce their radar cross section; in this case, the direct scattering problem amounts to a mixed boundary value problem with Maxwell's equations posed on an unbounded domain and where on the coated part of the boundary the electromagnetic field satisfies an impedance boundary condition while on the remaining part of the boundary the tangential component of the total electric field vanishes. An other domain of application is the use of this condition as an absorbing boundary condition to limit the computational domain of a finite elements method [2]. This condition plays also a major role in the domain decomposition methods for Maxwell's equations [3–5]. Thus, it appears crucial to have efficient numerical methods well suited for such boundary conditions. Although these IBC models are adequate for many numerical simulations, the way used to derive them implies a range of validity [30] and their use to model bounded materials can pose some problems because of the presence of breaks between the different materials. One can emphasize that the research of correct models to take into account this situation is still an open problem and that requires a fine comprehension of the behavior of the solution near breaks.

In the frequency domain, the total electromagnetic fields are expressed in terms of the equivalent electric and magnetic currents flowing on the surface of the scatterer, these currents being determined via the boundary condition. This is the basic principle of Boundary Integral Methods (BIM) which are often used to solve this kind of problems. It is known that different integral equations can be derived to get the currents and a first problem is to choose the good one. For the impedance problem, the main difficulty comes from the fact that the electric $\mathbf{J}$ and magnetic currents $\mathbf{M}$ are linked by a relation which it is difficult to take into account numerically. It is well known that the flux continuity of $\mathbf{M}$ and $\mathbf{J}$ across the edges of the mesh is crucial to ensure a "good" approximation. Generally, one directly imposes it in the approximate space. For example, one uses the Rao-Wilton-Glisson finite elements space (RWG) [6]. But, in this case, one cannot ensure the IBC in a strong way, since the flux continuity is not preserved when the application $\phi \rightarrow \mathbf{n} \times \phi$ is applied. For example, the finite elements space $\mathbf{n} \times \mathrm{RWG}$ only ensures a tangential continuity. To treat this difficulty, there are several possibilities. A first uses an integral formulation which only ensure the IBC when the convergence (i.e., when the spatial step tends toward zero) is achieved [9]. A second is to impose the IBC via a Lagrange multiplier [7]. Unfortunately,

these equations generally degenerate to an Electric Field Integral Equation (EFIE) when $\eta = 0$, i.e., for perfectly metallic part of Γ. Consequently, some problems can appear when one wants to treat partially coated objects for example. Indeed, it is known that the convergence rate of many iterative solvers is low for the EFIE. That is why, we have decided to study the possibility to use an equation like a Combined Field Integral Equation (CFIE). Since, one knows that this type of equation is well-conditioned for the perfectly metallic case. For this formulation, the IBC is imposed in a weak way and we have proposed some techniques to eliminate the magnetic current during the iterative process. Moreover, we will see that the choice of an adequate parameter β to combine the EFIE and Magnetic Field Integral Equation (MFIE) i.e., CFIE $=$ EFIE $+\,\beta$MFIE also leads to good iterative behaviors when the impedance operator is not equal to zero. Finally, our approach will avoid any additional development in comparison with the classical metallic CFIE in particular when one uses the Fast Multipole Computation.

The paper is divided as follows. In Section 2, we present the scattering problem to be solved. In Section 3, we first briefly introduce the classical techniques used to construct the boundary integral equations in electromagnetism and then we introduce a new technique based on a CFIE. We also explain the different difficulties induced by its implementation. Section 4 is devoted to the discretization of this method. In particular, some techniques to eliminate the magnetic current and to treat the rotation operator $n \times \cdot$ are described. In Section 5, we also propose a construction of a SPAI preconditioner associated to this formulation. Finally, in Section 6, some numerical experiments are exposed. A comparison with a well-tried method allows us to show the advantages of the proposed method in terms of robustness, memory storage and CPU time. In particular, we will see that it is particularly well adapted to treat the cases where the objects are only partially coated.

2. THE SCATTERING PROBLEM

Let Ω^- be a bounded open set of $\mathbb{R}^3$ with a smooth boundary Γ. The open complement of Ω^- in $\mathbb{R}^3$ is Ω^+. Vector **n** denotes the unit normal to Γ pointing into the exterior domain Ω^+ of Ω^-. The problem is to find the electromagnetic fields **E** and **H** solution to the time harmonic Maxwell system (with $e^{-i\omega t}$ time dependence)

$$
\begin{aligned}
\operatorname{rot} \mathbf{E} - ikZ_0\mathbf{H} &= 0 \text{ in } \Omega^+, \\
\operatorname{rot} \mathbf{H} + ikZ_0^{-1}\mathbf{E} &= 0 \text{ in } \Omega^+,
\end{aligned}
\tag{1}
$$

completed with both the Silver-Müller radiation condition at infinity [18] and the impedance boundary condition on the surface Γ

$$\mathbf{n} \times (\mathbf{E}_{|\Gamma} \times \mathbf{n}) - Z_0\eta\,(\mathbf{n} \times \mathbf{H}_{|\Gamma}) = 0. \tag{2}$$

Here, $k > 0$ is the wavenumber, Z_0 is the intrinsic impedance of the vacuum and $\eta(x)$ is an impedance function which is complex with a non negative real part. The variations of $\eta(x)$ allows us to take into account the presence of different materials on the surface Γ of the obstacle.

A strict positivity condition on the real part of η is required in the case where the scatterer is absorbing but also for theoretical reasons (well-posedness) [8]. In what follows, we suppose that the impedance operators considered verify this condition.

3. DERIVATION OF AN IMPEDANCE CFIE

3.1. Integral Representation of the Solution

Any electromagnetic field $(\mathbf{E}, \mathbf{H})$ in Ω^+ which is a sum of a plane wave $(\mathbf{E}^{\mathrm{inc}}, \mathbf{H}^{\mathrm{inc}})$ and of a radiating field is uniquely determined by the knowledge of the two equivalent currents,

$$\mathbf{J}(x) = \mathbf{n} \times \mathbf{H}_{|\Gamma}(x) \text{ and } \mathbf{M}(x) = -\frac{1}{iZ_0}\mathbf{n} \times \mathbf{E}_{|\Gamma}(x)^\dagger, \tag{3}$$

through the well known Stratton-Chu formulae [10],

$$\begin{cases} \mathbf{E}(x) = \mathbf{E}^{\mathrm{inc}}(x) + iZ_0\big(\tilde{T}\mathbf{J}(x) + \tilde{K}\mathbf{M}(x)\big) \ x \in \Omega^+ \\[2mm] \mathbf{H}(x) = \mathbf{H}^{\mathrm{inc}}(x) - \tilde{K}\mathbf{J}(x) - \tilde{T}\mathbf{M}(x) \ x \in \Omega^+, \end{cases} \tag{4}$$

where the respective potentials $\tilde{T}$ and $\tilde{K}$ are defined by

$$\begin{cases} \tilde{T}\mathbf{J}(x) = k \int_\Gamma G(x,y)\mathbf{J}(y)d\Gamma(y) \\[2mm] \qquad\quad +\dfrac{1}{k} \int_\Gamma \vec{\nabla}_x G(x,y)\mathrm{div}_\Gamma \mathbf{J}(y)d\Gamma(y) \\[2mm] \tilde{K}\mathbf{J}(x) = \int_\Gamma \vec{\nabla}_y G(x,y) \times \mathbf{J}(y)d\Gamma(y). \end{cases} \tag{5}$$

$G(x,y)$ is the Green kernel for the radiating solution of the 3-D Helmholtz equation and $\mathrm{div}_\Gamma\mathbf{J}$ denotes the surface divergence of $\mathbf{J}$.

The tangential traces on Γ of the potentials $\tilde{T}$ and $\tilde{K}$ are known; when x in Ω^+ approaches the boundary Γ in (4), we get [10],

$$
\begin{cases}
-(\mathbf{n} \times (\mathbf{E}^{\text{inc}})_{|\Gamma} \times \mathbf{n})(x) = iZ_0\big(T\mathbf{J}(x) + K\mathbf{M}(x) \\
\qquad\qquad\qquad -\dfrac{1}{2}\mathbf{n} \times \mathbf{M}(x)\big) \quad (6a) \\
(\mathbf{n} \times (\mathbf{H}^{\text{inc}})_{|\Gamma} \times \mathbf{n})(x) = +K\mathbf{J}(x) + T\mathbf{M}(x) \\
\qquad\qquad\qquad -\dfrac{1}{2}\mathbf{n} \times \mathbf{J}(x) \qquad (6b)
\end{cases}
\tag{6}
$$

where T and K are defined by

$$
T\mathbf{J}(x) = \lim_{y \to x} \mathbf{n}(x) \times (\tilde{T}\mathbf{J}(y) \times \mathbf{n}(x)),
$$

$$
K\mathbf{J}(x) = \left(\int_\Gamma \mathbf{n}(x) \times (\nabla_y G(x,y) \times \mathbf{J}(y)) d\Gamma(y) \right) \times \mathbf{n}(x) \tag{7}
$$

These two relations hold whatever the boundary condition on Γ is. There are not independent: except for some exceptional values of k (interior resonance), they are indeed equivalent. When impedance boundary condition is considered, we have to add the boundary condition (2) or equivalently

$$
\mathbf{n} \times \mathbf{M}(x) = -i\eta\,\mathbf{J}(x) \tag{8}
$$

The two unknowns $\mathbf{J}, \mathbf{M}$ have to be determined using the previous equations. Several boundary integral equations can be constructed to determine the currents, all of them amounts to combine (6) and (8) to get an equation with a unique solution. The derivations of some of these equations can be found for example in [7]. In particular, there exists a efficient method using the two currents as unknowns and in which the impedance condition is imposed in a implicit way [9, 7, 25]. In what follows, BGLF will denote this method. We will use BGLF to evaluate the new technique that we are going to propose. The main drawback of BGLF is that it degenerates into an EFIE on the metallic objects nevertheless at our knowledge, it is currently the most efficient method to solve the impedance problems.

3.2. An Impedance Combined Field Integral Equation Formulation (ICFIE)

It is well known that, in the case of perfectly metallic object, the CFIE leads to linear systems that can be solved by iterative methods with

a good convergence rate. That is why, we have decided to construct a CFIE to solve the impedance problem that we have considered. We expect that the good convergence rate for the CFIE will remain true for the impedance case.

We use a simple combination of (6) and (8) to derive our Impedance Combined Field Integral Equation formulation (ICFIE). More precisely, we normalize (6a) by Z_0 then apply a rotation of $\dfrac{\pi}{2}$ around the normal to (6b) (i.e., $\mathbf{n} \times \cdot$)

$$\begin{cases} -\dfrac{1}{Z_0}(\mathbf{n}\times(\mathbf{E}_{|\Gamma}^{\text{inc}} \times \mathbf{n}))(x) = i\left(T\mathbf{J}(x) + K\mathbf{M}(x)-\dfrac{1}{2}\mathbf{n} \times \mathbf{M}(x)\right) \\ (\mathbf{n} \times \mathbf{H}_{|\Gamma}^{\text{inc}})(x) = +\mathbf{n} \times K\mathbf{J}(x) + \mathbf{n} \times T\mathbf{M}(x) + \dfrac{1}{2}\mathbf{J}(x) \end{cases}$$

(9)

and we make a linear combination of these two equations

$$\begin{cases} -\dfrac{1}{Z_0}(\mathbf{n} \times (\mathbf{E}_{|\Gamma}^{\text{inc}} \times \mathbf{n}))(x) + \beta(\mathbf{n} \times \mathbf{H}_{|\Gamma}^{\text{inc}})(x) \\ = i\left(T\mathbf{J}(x) + K\mathbf{M}(x) - \dfrac{1}{2}\mathbf{n} \times \mathbf{M}(x)\right) \\ + \beta\left(\mathbf{n} \times K\mathbf{J}(x) + \mathbf{n} \times T\mathbf{M}(x) + \dfrac{1}{2}\mathbf{J}(x)\right). \end{cases}$$

(10)

This equation is commonly called in the literature the CFIE [7, 26].

We get the ICFIE system

$$\begin{cases} -\dfrac{\mathbf{E}_t^{\text{inc}}}{Z_0} + \beta\mathbf{n} \times \mathbf{H}_t^{\text{inc}} = \left(iT + \beta\mathbf{n} \times K + \dfrac{\beta}{2}\right)\mathbf{J} \\ \qquad\qquad -i\beta\mathbf{n} \times \left(iT + \dfrac{1}{\beta}\mathbf{n} \times K + \dfrac{1}{2\beta}\right)\mathbf{M} \\ 0 = i\eta\,\mathbf{J} + \mathbf{n} \times \mathbf{M}. \end{cases}$$

(11)

If $A_{cfie}^{\xi} = iT + \xi\mathbf{n}\times K + \frac{\xi}{2}$ denotes the classical integral operator for the CFIE in the metallic case, we remark that the two integral operators involved in the first equation of (11) are simply A_{cfie}^{β} and $A_{cfie}^{\frac{1}{\beta}}$; we have

$$\begin{cases} -\dfrac{\mathbf{E}_t^{\text{inc}}}{Z_0} + \beta\mathbf{n} \times \mathbf{H}_t^{\text{inc}} = A_{cfie}^{\beta}\mathbf{J} - i\beta\mathbf{n} \times A_{cfie}^{\frac{1}{\beta}}\mathbf{M} \\ 0 = i\eta\,\mathbf{J} + \mathbf{n} \times \mathbf{M} \end{cases}$$

(12)

Note that (12) can not straightforwardly be discretized by a finite elements method. Indeed, if one multiplies the first equation of (12) by a test function $\mathbf{J}'$, one must be able to evaluate both $(T\mathbf{J}, \mathbf{J}')$ and $(\mathbf{n} \times T\mathbf{M}, \mathbf{J}')$ in the same fashion. In particular, after an integration by parts, one must correctly approximate two terms:

$$A_1 = \int_\Gamma \int_\Gamma G(x,y) div_\Gamma \mathbf{J}(y) \operatorname{div}_\Gamma \mathbf{J}'(x) d\Gamma(y) d\Gamma(x)$$

$$A_2 = \int_\Gamma \int_\Gamma G(x,y) div_\Gamma \mathbf{M}(y) \operatorname{div}_\Gamma (\mathbf{n} \times \mathbf{J}'(x)) d\Gamma(y) d\Gamma(x) \quad (13)$$

So, $\operatorname{div}_\Gamma \mathbf{J}'$ and $\operatorname{div}_\Gamma(\mathbf{n} \times \mathbf{J}') = curl_\Gamma \mathbf{J}'$ must be defined. Consequently, $\mathbf{J}'$ must rigorously belong to a finite elements space where the tangential and normal continuity are ensured. To our knowledge, no finite-element method is yet available which, while remaining simple enough, at the same time satisfies such a degree of continuity constraint and applies to a surface of arbitrary shape.

In order to overcome this difficulty two simple ways to approach $(\mathbf{n} \times T\mathbf{M}, \mathbf{J}')$ (and consequently $(\mathbf{n} \times A_{cfie}^{\frac{1}{\beta}}\mathbf{M}, \mathbf{J}'))$ **without new developments** for the integral operators are proposed in this paper. More precisely, only the discretization of CFIE operator $A_{cfie}^{\frac{1}{\beta}}$ is needed. These two techniques are based on projections on classical finite elements spaces.

The first choice is natural and intuitive. We first decide to determine an approximate $\mathcal{V} \in$ RWG of $A_{cfie}^{\frac{1}{\beta}}\mathbf{M}$ and then simply compute $(\mathbf{n} \times \mathcal{V}, \mathbf{J}')$. It can be formally described by the augmented system noted by the ICFIE1 system

$$\begin{cases} -\dfrac{\mathbf{E}_t^{\text{inc}}}{Z_0} + \beta\mathbf{n} \times \mathbf{H}_t^{\text{inc}} = A_{cfie}^{\beta}\mathbf{J} - i\beta\mathbf{n} \times \mathcal{V} & \text{(a1)} \\[2mm] \mathcal{V} = A_{cfie}^{\frac{1}{\beta}}\mathbf{M} & \text{(b1)} \\[2mm] \mathbf{n} \times \mathbf{M} = -i\eta\mathbf{J} & \text{(c1)} \end{cases} \quad (14)$$

The second choice appears when one interests to how the operator T acts on functional spaces. It is well known that the range of T is included in $H^{-1/2}(curl_\Gamma, \Gamma)$ [18] where

$$H^{-\frac{1}{2}}(curl_\Gamma, \Gamma) = \{(\mathbf{n} \times (\mathbf{u} \times \mathbf{n}))_{|\Gamma} : \forall \mathbf{u} \text{ such that } \mathbf{u}, \nabla \times \mathbf{u} \in [L^2(\Omega^-)]^3\}$$

In this space, the $curl_\Gamma$ operator is well-defined and consequently one has the tangential continuity. So, if one wants to respect the functional

framework $(T\mathbf{M} \in H^{-\frac{1}{2}}(curl_\Gamma, \Gamma))$, it is natural to approach $T\mathbf{M}$ by an element belonging to a finite elements space which ensures such continuity. It is not the case in the first technique where $T\mathbf{M}$ is approached by an element of RWG for which only the normal flux continuity is ensured. The first idea is to find $V \in \mathbf{n} \times \text{RWG} \approx TM$ since $\mathbf{n} \times \text{RWG}$ is a subspace of $H^{-1/2}(curl_\Gamma, \Gamma)$. This consists to solve the problem: find $V = \mathbf{n} \times W \in \mathbf{n} \times \text{RWG}$ such that $\forall W' \in \text{RWG}$, $\int_\Gamma \mathbf{n} \times W \cdot W' d\Gamma = (T\mathbf{M}, W')$. But, it is well-known that the left integral leads to a non-invertible matrix. In [15], it is proposed a technique which allows to correctly realize such duality. We will briefly describe it in IV-B and we will then explain how to use it. This second technique can be formally described by the augmented system noted by the ICFIE2 system

$$\begin{cases} -\dfrac{\mathbf{E}_t^{\mathrm{inc}}}{Z_0} + \beta \mathbf{n} \times \mathbf{H}_t^{\mathrm{inc}} = A_{cfie}^{\beta}\mathbf{J} - i\beta X & \text{(a2)} \\[2mm] \mathbf{n} \times X = -A_{cfie}^{\frac{1}{\beta}}\mathbf{M} & \text{(b2)} \\[2mm] \mathbf{n} \times \mathbf{M} = -i\eta\mathbf{J} & \text{(c2)} \end{cases} \qquad (15)$$

One can ask the question: why to have kept the first approach? In fact, we will see that the first technique provides an interesting response in practice. Moreover, it can be easy and quickly implemented.

Finally, note that after discretization, it is easy to compute a matrix-vector product $A_{cfie}^{\beta}\mathbf{J}$ and $A_{cfie}^{\frac{1}{\beta}}\mathbf{M}$, using twice times, the FMM algorithm applied to the "classical" CFIE equation.

Remark: Another process, denoted by ICFIE3 in the following, can also be considered; it is based on the following system of equations

$$\begin{cases} -\dfrac{\mathbf{E}_t^{\mathrm{inc}}}{Z_0} + \beta \mathbf{n} \times \mathbf{H}_t^{\mathrm{inc}} = A_{cfie}^{\beta}\mathbf{J} + \left(\beta \mathbf{n} \times T + iK - \dfrac{i}{2}\mathbf{n} \times\right)\mathbf{M} & \text{(b3)} \\[2mm] \mathbf{n} \times \mathbf{M} = -i\eta\mathbf{J} & \text{(c3)} \end{cases} \qquad (16)$$

Indeed, one can numerically evaluate A_2 (13) all the same and it is even the classical way to compute $\mathbf{n} \times T$. For that, one writes $div_\Gamma(\mathbf{n} \times \mathbf{J}')$ in this way

$$div_\Gamma(\mathbf{n} \times \mathbf{J}') = \begin{cases} div_{K_i}(\mathbf{n} \times \mathbf{J}'_{|K_i}) & \text{on triangle } K_i \\[2mm] (\mathbf{J}'^j \cdot \nu^{ij} + \mathbf{J}'^i \cdot \nu^{ji})\delta_{ij} & \text{on } \overline{K}_i \cap \overline{K}_j \end{cases} \qquad (17)$$

where δ_{ij} is the Dirac measure associated to the edge $\overline{K}_i \cap \overline{K}_j$ of the mesh, ν^{ij} is the unit outward normal to $\overline{K}_i \cap \overline{K}_j$ and tangential to

K_i, div_{K_i} is the surface divergence operator computed on the K_i and $\mathbf{J}'^j = \mathbf{J}'_{|K_j}$ (the same thing for i).

Now, splitting up A_2 on each triangle and using (17), one obtains for sufficiently smooth tangential vector fields on each triangle

$$
\begin{aligned}
A_2 &= \sum_{K_i} \int_{K_i} \int_{\Gamma} G(x,y)\mathrm{div}_{\Gamma}\mathbf{J}(y)\mathrm{div}_{K_i}(\mathbf{J}'(x) \times \mathbf{n}(x))d\Gamma(y)d\Gamma(x) \\
&\quad + \sum_{\overline{K}_i \cap \overline{K}_j} \int_{\overline{K}_i \cap \overline{K}_j} \int_{\Gamma} G(x,y)\mathrm{div}_{\Gamma}\mathbf{J}(y)((\mathbf{J}'^j \times \mathbf{n}_j) \cdot \nu^{ij} \\
&\quad + (\mathbf{J}'^i \times \mathbf{n}_i) \cdot \nu^{ji})d\Gamma(y)dA_{ij}(x)
\end{aligned}
\tag{18}
$$

where dA_{ij} is the linear measure of the edge $\overline{K}_i \cap \overline{K}_j$ and $\mathbf{n}_{i\,\mathrm{ou}\,j} = \mathbf{n}_{|K_{i\,\mathrm{ou}\,j}}$.

Formula (18) shows that one can now calculate the term $\mathbf{n} \times T$ after discretization by the RWG finite elements. However, even if this approach may be possible, it presents a drawback when multipoles are considered: since the new formulation involves integral over edges in addition to integrals over triangles, we will have to compute far fields with respect to clusters of Gauss points located on edges in addition to the classical far fields with respect to Gauss points located to triangles, what will imply a cost multiplied by 2. This is why we decide to give up this formulation. However, it will appear to be useful to construct a preconditioner (see Section 5.1).

4. DISCRETE SCHEME

The discrete problem is obtained by means of Galerkin's method; the scatterer's surface Γ is meshed with triangles, and the surface electric and magnetic currents are expanded as $\mathbf{J}(x) \simeq \mathbf{J}^h(x) = \sum_{j=1}^{N} J_j^h \phi_j(x)$ and $\mathbf{M}(x) \simeq \mathbf{M}^h(x) = \sum_{j=1}^{N} M_j^h \phi_j(x)$, where the $\phi_j(x)$'s are the RWG basis functions associated to the mesh [6].

In the following, J^h (resp. M^h) denotes the column vector which contains the degrees of freedom of the electric current (resp. magnetic current).

4.1. Discretization of the ICFIE1

We consider first the system given by (14). The new auxiliary variable $\mathcal{V}$ is also approximated by a element in RWG. Vector V^h corresponds to the column vector which contains the degrees of freedom of $\mathcal{V}$. The

discretization is proceeded in the usual way. It leads to a linear system in the unknowns (J^h, M^h, V^h). Different steps can be drawn

(a)-Discretization of the operator $A^\beta_{cfie} = iT + \beta \mathbf{n} \times K + \dfrac{\beta}{2}$:

The term $\left(iT + \beta\mathbf{n} \times K + \dfrac{\beta}{2}\right)\mathbf{J}$ is transformed into $\mathcal{A}^\beta_{h,cfie}J^h$ where $\mathcal{A}^\beta_{h,cfie}$ is the usual matrix of the interactions between the basis functions for the $CFIE$ equation in the metallic case:

$$
\begin{aligned}
\left(\mathcal{A}^\beta_{h,cfie}\right)_{i,j} =\ & ik \int_\Gamma \int_\Gamma G(x,y)\big(\phi_i(x) \cdot \phi_j(y) \\
& -\frac{1}{\kappa^2}\vec{\nabla}_\Gamma \cdot \phi_j \vec{\nabla}_\Gamma \cdot \phi_i\big)d\Gamma(x)d\Gamma(y) \\
& +\frac{\beta}{2}\int_\Gamma \phi_j(x) \cdot \phi_i(x)d\Gamma(x) \\
& +\beta\int_\Gamma\int_\Gamma \nabla_y G(x,y)\times\phi_j(y)\cdot(\phi_i(x)\times n(x))d\Gamma(y)d\Gamma(x)\ (19)
\end{aligned}
$$

(b)-Elimination of the magnetic current (see Equation (c1) of (14)):

The first idea to determine the current $\mathbf{M}^h$ when $\mathbf{J}^h$ is assumed to be known, is to project the impedance condition directly onto the space $\mathbf{n} \times$ RWG: for all test functions in RWG, Equation (c1) of (14) leads to

$$
\begin{aligned}
\int_\Gamma \mathbf{M}^h \cdot \mathbf{M}'d\Gamma &= \int_\Gamma (\mathbf{n} \times \mathbf{M}^h) \cdot (\mathbf{n} \times \mathbf{M}')d\Gamma \\
&= -i\int_\Gamma \eta\mathbf{J}^h \cdot (\mathbf{n} \times \mathbf{M}')d\Gamma, \quad\quad (20)
\end{aligned}
$$

which corresponds to the following matrix relationship between the discrete electric and magnetic currents

$$
\mathcal{M}_h M^h = -i\mathcal{M}^\eta_{div/rot,h} J^h \quad\quad (21)
$$

$\mathcal{M}_h$ is the mass matrix of the finite elements space $\mathbf{n} \times$ RWG while $\mathcal{M}^\eta_{div/rot,h}$ is the matrix

$$
\left(\mathcal{M}^\eta_{div/rot,h}\right)_{i,j} = \int_\Gamma \eta\phi_i \cdot (\mathbf{n} \times \phi_j)d\Gamma.
$$

(c)-Discretization of the the operator $A^{\frac{1}{\beta}}_{cfie}$:

Multiplying Equation (b1) of (14) by a RWG basis function and

integrating over the surface, we obtain a relation between V^h and M^h,

$$\mathcal{M}_h V^h = \mathcal{A}_{cfie,h}^{\frac{1}{\beta}} M^h \qquad (22)$$

Knowing V^h, all that is left to do is to carry out the sparse matrix-vector product $\mathcal{M}_{rot/div,h} V_h$ where $\mathcal{M}_{rot/div,h}$ is the matrix of the interactions $(\mathbf{n} \times \phi_i, \phi_j)$.

Formally, we can write the system corresponding to the solution of the ICFIE1 by using the steps **(a)**, **(b)** and **(c)**:

$$\left(\mathcal{A}_{cfie,h}^{\beta} - \beta \mathcal{M}_{rot/div,h} \mathcal{M}_h^{-1} \mathcal{A}_{cfie,h}^{\frac{1}{\beta}} \mathcal{M}_h^{-1} \mathcal{M}_{div/rot,h}^{\eta} \right) J^h = B^{inc,h}, \quad (23)$$

where the vector column $B^{inc,h}$ corresponds to the second member. We solve system (23) by an iterative solver with J^h as the only unknown. Both the magnetic current M^h and the auxiliary variable V^h are eliminated during the matrix-vector product needed at each iteration by using the strategy **(b)** and **(c)**. Systems (21) and (22) can be solved by means of a sparse solver which allows a quick and low cost inversion. In our numerical experiments, we have used MUMPS [19], (i.e., Multifrontal Massively Parallel sparse direct Solver). The matrix vector products involving the matrices $\mathcal{A}_{cfie,h}^{\beta}$ and $\mathcal{A}_{cfie,h}^{\frac{1}{\beta}}$ are performed using the Multilevel Fast Multipole Method [23, 24]. We have chosen GMRES as our iterative solver (more precisely, we use the free GMRES solver described in [14]). GMRES is known to be the iterative method with the minimal rate of convergence.

4.2. Discretization of the ICFIE2 System (15)

We now described the technique proposed in [15] in order to do an efficient approximation of $n \times A_{cfie}^{\frac{1}{\beta}}$. This technique is based on a discrete analogue of the Helmholtz decomposition of the tangential fields. Let us recall the Helmholtz decomposition of a tangential field $\mathbf{u}$ of Γ [27]:

$$\mathbf{u} = \mathbf{u}_1 + \mathbf{u}_2$$

where $\mathrm{div}_\Gamma \mathbf{u}_1 = \mathrm{curl}_\Gamma \mathbf{u}_2 = 0$.

The idea of [15] is to separately carried out the rotation $(\mathbf{n} \times \cdot)$ of $\mathbf{u}_1$ and $\mathbf{u}_2$ in order to obtain a mathematically stable evaluation of $\mathbf{n} \times \mathbf{u}$. The technique is completely analyzed in [15]. We are going only to explain the different steps:

Let l_h be a linear form defined on RWG; the problem is to construct some $\Theta^h l_h$ that mimics $\mathbf{n} \times l_h$. In what follows, P_0^o denotes the space of scalar functions whose restriction to any triangle is constant and whose mean value is null on Γ and P_1^o denotes the space of scalar functions, piecewise linear on each triangle of the mesh and whose mean value is null on Γ.

- First, we consider the following saddle-point problem:
  Find $(u^h, q^h) \in RWG \times P_0^o$ *such that for all* $(u', q') \in RWG \times P_0^o$,

$$
\begin{cases}
\displaystyle\int_\Gamma u^h \cdot u' d\Gamma + \int_\Gamma q^h \operatorname{div} u' d\Gamma = l^h(u') \\[2mm]
\displaystyle\int_\Gamma q' \operatorname{div} u^h d\Gamma = 0.
\end{cases}
\tag{24}
$$

  (24) realizes an discrete Helmholtz decomposition of l_h. Indeed, one can formally write that $l_h = u^h - (\nabla_\Gamma)^* q^h$ where $\operatorname{div} u^h = 0$ and $((\nabla_\Gamma)^* q^h, u') = -\int_\Gamma q^h \operatorname{div} u' d\Gamma$. $(\nabla_\Gamma)^* q^h$ approaches the curl-free part of the exact linear form l.

- Once this system is solved, we associate to (u^h, q^h) the following element of RWG :

$$
v^h = \Theta^h l^h = \mathcal{P}_{RWG}(u^h \times \mathbf{n}) - \mathbf{n} \times \nabla \mathcal{P}_{P_1^o}(q^h),
\tag{25}
$$

  where $\mathcal{P}_X$ denotes the L²-projection on the finite element space X.
  $\mathcal{P}_{RWG}(u^h \times \mathbf{n})$ gives an approximation in RWG of the rotation of the divergence-free part and $\mathbf{n} \times \nabla \mathcal{P}_{P_1^o}(q^h)$ an approximation of the rotation of the curl-free part. So v_h is an approximation of $l^h \times \mathbf{n}$ in RWG.
  We use twice the linear operator Θ^h to construct our ICFIE:

- We take $l^h(u') = \int_\Gamma \eta \mathbf{J}^h \cdot u' d\Gamma = \mathcal{M}_h^\eta \mathbf{J}^h$ and $M^h = -i\Theta^h l^h$ provides us the magnetic current.

- We take $l^h(u') = (\mathcal{A}_{cfie}^{1/\beta} \mathbf{M}^h, u')$ and $\Theta^h l^h$ corresponds to an approximation of the unknown X in (25). Then, we simply compute the product $\int_\Gamma \Theta^h l^h \cdot \mathbf{J}' d\Gamma$ to obtain the discrete equivalent to $(\mathbf{n} \times \mathcal{A}_{cfie}^{1/\beta} \mathbf{M}^h, \mathbf{J}')$.

Finally, we get the system

$$
\left(\mathcal{A}_{cfie,h}^\beta - \beta \mathcal{M}_h \Theta_h \mathcal{A}_{cfie,h}^{\frac{1}{\beta}} \Theta_h \mathcal{M}_h^\eta \right) J^h = B^{inc,h},
\tag{26}
$$

One possesses two techniques to carry out the intermediate computations in order to obtain the ICFIE formulation. Both are

solved by using the sparse solver MUMPS, but one can see the latter requires more inversions (i.e., solution of (24) and two projections in (25) $\Rightarrow$ two additional inversions whereas the first only requires one inversion). From numerical experiments, we will show that the second technique allows to obtain a more accurate solution.

5. ITERATIVE SOLUTION

5.1. SParse Approximate Inverse (SPAI) Preconditioner for the ICFIE Formulation

To speed up the convergence of our iterative solver, we construct a right preconditioner following [17, 28]. Its design follows the following lines: first, we scatter the degrees of freedom into n_b boxes. The side length of the boxes is generally taken to be a fraction of the wavelength. If B is a box, we define, $\mathcal{V}(B)$, the set of the neighboring boxes of B (B included) and $\mathcal{V}^2(B)$ the set of boxes B' for which it exists a box b such that both B and B' are in $\mathcal{V}(b)$. We fix the profile of the preconditioner as the set of the (j, k)'s with j in $\mathcal{V}(B)$ with B the box of k. The coefficients of the preconditioner $p_{j,k}$ are defined by

$$p = \operatorname{Argmin} \left(\sum_B \sum_{k \in B} \sum_{i \in \mathcal{V}^2(B)} \left(\delta_i^k - \sum_{j \in \mathcal{V}(B)} a_{i,j} p_{j,k} \right)^2 \right).$$

The solution can be found by solving n_b independent least square problems: let n_{dof}^b be the number of degrees of freedom located inside box b; if B is a given box, the number of linear equations of the associated least square problem is $n_{dof}^B \times \sum_{b \in \mathcal{V}^2(B)} n_{dof}^b$ while the number of unknowns is $n_{dof}^B \times \sum_{b \in \mathcal{V}(B)} n_{dof}^b$.

The main difficulty to construct a sparse inverse of systems (23) and (26) is the presence of the inverses of some matrices. If we want to take into account them exactly, we have to increase the size of the system by a number of unknowns equals to the number of inversions. For example, the system (23) would be rewritten in form:

$$\begin{pmatrix} \mathcal{A}_{cfie,h}^{\beta} & -i\beta\mathcal{M}_{rot/div,h} & 0 \\ 0 & \mathcal{M}_h & -\mathcal{A}_{cfie,h}^{\frac{1}{\beta}} \\ i\mathcal{M}_{div/rot,h}^{\eta} & 0 & \mathcal{M}_h \end{pmatrix} \begin{pmatrix} J^h \\ U^h \\ M^h \end{pmatrix} = \begin{pmatrix} B^{inc,h} \\ 0 \\ 0 \end{pmatrix}$$

(27)

If we represent the sparse inverse of (27) by the block matrix

$$\begin{pmatrix} P_{11} & P_{12} & P_{13} \\ P_{21} & P_{22} & P_{23} \\ P_{31} & P_{32} & P_{33} \end{pmatrix}, \tag{28}$$

the term P_{11} is a preconditioner for (23). If one considers system (26) corresponding to ICFIE2, the size of the equivalent system (27) becomes larger. To avoid this problem, we have decided to construct the preconditioner of ICFIE1 and ICFIE2 by using the matrix which is derived from the ICFIE3 system (16). It is legitimate to think that this choice is sufficient to construct an "approximate" inverse. With regards to the elimination of the magnetic current, we keep the process (21). Indeed, it is judicious to keep it since as we have specified above a direct elimination of $\mathbf{M}$ via the impedance condition poses problems. Finally, we compute a sparse inverse of the system:

$$\begin{pmatrix} \mathcal{A}^{\beta}_{cfie,h} & \mathcal{Z}^{M}_{h} \\ i\mathcal{M}^{\eta}_{div/rot,h} & \mathcal{M}_{h} \end{pmatrix} \begin{pmatrix} J^{h} \\ M^{h} \end{pmatrix} = \begin{pmatrix} B^{inc,h} \\ 0 \end{pmatrix} \tag{29}$$

where $\mathcal{Z}^{M}_{h}$ corresponds to the direct discretization of the operator $\beta\mathbf{n} \times T + iK - \dfrac{i}{2}\mathbf{n}\times$.

5.2. Algorithm

This part describes the main steps of the algorithm of the ICFIE:

- Calculation of the preconditioner and storage on disc.

- Calculation of close matrices for the $\mathcal{A}^{\beta}_{cfie,h}J^{h}$ and the $\mathcal{A}^{\frac{1}{\beta}}_{cfie,h}M^{h}$ which are needed by the FMM algorithm and storage on disc.

- Calculation of matrices which are necessary to the elimination of $\mathbf{M}$ and to do the matrix-vector product corresponding to $\mathbf{n} \times \mathcal{V}$ or $\mathbf{n} \times X$.

- For each iteration:
  - Calculation of M^{h} ($M^{h} = -i\mathcal{M}^{-1}_{h}\mathcal{M}^{\eta}_{div/rot,h}J^{h}$ or $M^{h} = \Theta_{h}\mathcal{M}^{\eta}_{h}J^{h}$),
  - Calculation of $\mathcal{A}^{\frac{1}{\beta}}_{cfie,h}M^{h}$ by using a two components fast multipole algorithm,
  - Calculation of $\mathbf{n} \times \mathcal{V}$ or X,
  - Calculation of $\mathcal{A}^{\beta}_{cfie,h}J^{h}$ by using a two components fast multipole algorithm.

Remark: Let us make a remark on the memory storage for the BGLF and the ICFIE. When one uses a FMM, the main storage comes from the preconditioner and the close matrices:

- For the preconditioner, if we denote by α_p the number of neighbors by electric degree of freedom, the required memory is $(\alpha_p N + \alpha_p N)2 = 4\alpha_p N$ complex numbers (where N is the number of electric degrees of freedom) for BGLF (because there are two currents $\mathbf{J}$ an $\mathbf{M}$) and $\alpha_p N$ complex numbers for the ICFIE.

- For the close matrices, if we denote by α_c the number of neighbors by electric degree of freedom, the required memory is $(\alpha_c N + \alpha_c N)2/2/2 = \alpha_c N$ real numbers for BGLF (the first division by 2 corresponds to the necessity to store uniquely the real part and the second comes from the symmetry of the system) and $2\alpha_c N$ complex numbers for the ICFIE (the factor 2 is due to the fact that we have the two dense matrices A_{cfie}^{β} and $A_{cfie}^{\frac{1}{\beta}}$).

Denote $\alpha = \dfrac{\alpha_c}{\alpha_p}$, we obtain global memory storages equal to $N\alpha_p(8 + \alpha)$ for BGLF and $2\alpha_p N(1 + 2\alpha)$ for ICFIE. This implies the ratio

$$\frac{\text{BGLF memory}}{\text{ICFIE memory}} = \frac{8 + \alpha}{2(1 + 2\alpha)}$$

which belongs to the interval $]\dfrac{1}{4}; 2[$. In the next section, we will be able to see that it is equal to 1.5 for the case of the sphere. To finish, we point out to the reader that the two methods have not the same degree of maturity and that ICFIE may be surely improved with regard to the close matrix.

6. NUMERICAL EXPERIMENTS

In this section, several numerical experiments are presented to show the ability of the ICFIE method to effectively solve an impedance problem. To carry out this work, a comparison is done with results obtained using BGLF, which is a well-tried numerical method to solve this kind of problems. The frame of this analysis is the following:

- Cost of the preconditioner: we evaluate the density (the number of non-zero values divided by the square of the number of unknowns) and the CPU time of construction of the preconditioner.

- Accuracy: in order to quantify the accuracy of our new formulations, we compare the result obtained with the reference

solution and compute the relative errors between the two solutions. The reference solution can be in some cases analytical or given by the BGLF.

- Robustness and cost: we evaluate the robustness (number of iterations necessary to obtain a solution with a residual equal to 10^{-4}) and the CPU time spent for different values of the impedance.

For all examples, the discretization complies with the criterion of around 10 points per wavelength. We consider three scattering objects illuminated by a plane wave with a wavenumber k:

- **Object 1**: A sphere of radius $1\,\mathrm{m}$. Its mesh is made of 338000 triangles that corresponds to 507000 edges.We have fixed the wavenumber equal to $k = 63\,\mathrm{m}^{-1}$. Three impedance values will be considered:
  - Case 1: $\eta = 1$
  - Case 2: $\eta = 8.55 \cdot 10^{-2}(1 + i)$
  - Case 3: $\eta = 0.34 + 0.29i$
- **Object 2**: A cube whose the mesh is composed of 3240 triangles.The wavenumber k is equal to $15.82\,\mathrm{m}^{-1}$ and $\eta = 1$.
- **Object 3**: A cylinder of height $360\,\mathrm{m}$ and radius $120\,\mathrm{m}$. The mesh is composed of 347324 triangles that corresponds to 520986 edges. The wavenumber is fixed to $k = 0.63\,\mathrm{m}^{-1}$ and we have considered two configurations which are summed up in Table 1. The first one corresponds to a constant impedance while, in the second one, we have divided the cylinder in three sections with three distinct values of the impedance. In particular, one of the sections is assumed to be perfectly conducting ($\eta = 0$). For this example, the GMRES residual is equal to 10^{-3}.

Table 1. Case description.

case	η		
case 1	0.34 + 0.29i		
case 2	0.34 + 0.29i $0 < z < 120$	0. $120 < z < 240$	0.34 + 0.29i $240 < z < 360$

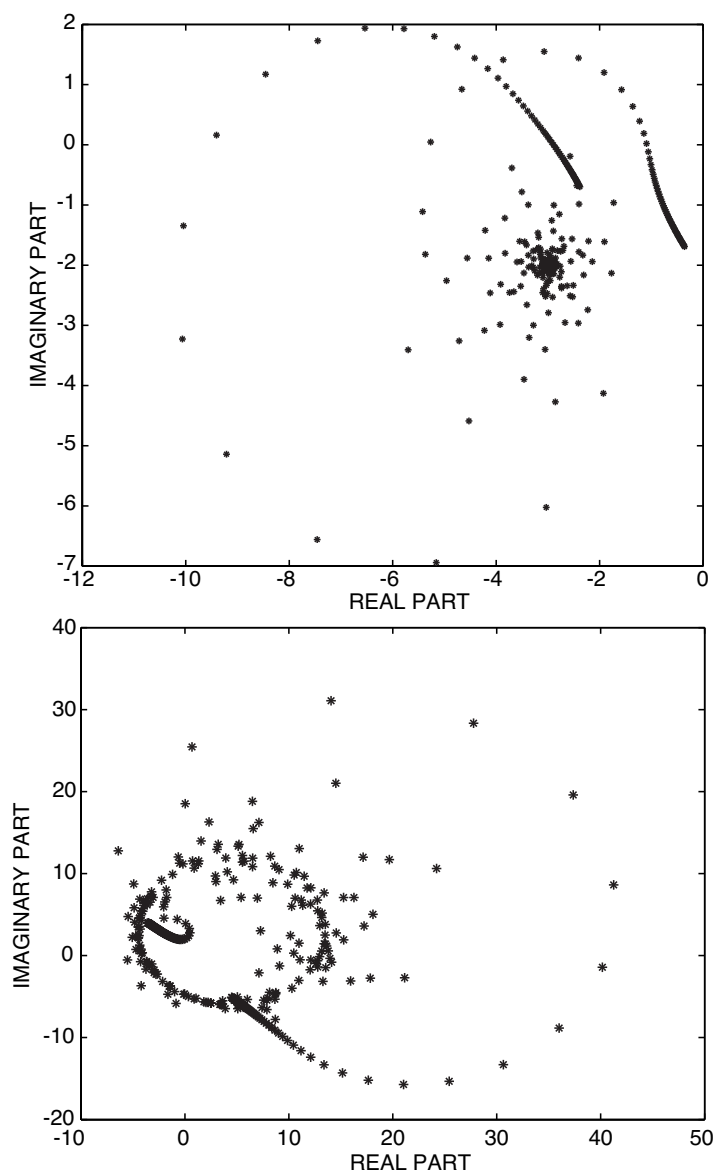In what follows, objecti-j denotes that we treat the case j of the object i.

Figure 1. Spectrum in the case of the sphere of radius a with a constant impedance $\eta = 2 + 2i$ and $ka = 100$. The up panel is for $\beta = -1$, the down panel for $\beta = 4$.

6.1. Choice of the Parameter β

β acts upon both the robustness and the accuracy of the scheme. For the perfectly metallic case, it is commonly admitted that $\beta = 4$ is, in most cases, the best compromise. It is not clear that this value remains still the best choice for the impedance condition. In fact, it is not the case. On can prove theoretically on spherical geometry that $\beta = -1$ allows the best clustering of eigenvalues of the ICFIE system in the complex plane [12]. Figure 1 clearly shows the bringing together around a point of the eigenvalues for the case $\beta = -1$ whereas for $\beta = 4$ the spectrum is more dispersed and turns around the origin. In terms of iterative performance, we have subjected these systems of eigenvalues to a GMRES solver. Table 2 sums up the number of iterations obtained for $\eta = 2+2i$ and several values of the wavenumber. The value $\beta = -1$ seems to be a good choice for the robustness. Moreover, it is well known that the MFIE term penalizes the CFIE in term of accuracy. The choice $\beta = -1$ is *a priori* less penalizing than $\beta = 4$.

Table 2. Number of iterations (residual less than 10^{-5}).

η=2+2i	$\beta = -1$	β=4
ka =5	19	28
ka =10	28	54
ka =100	39	241

Table 3 contains the number of iterations needed to obtain the solution for Object1-3 and Object3-2 and for $\beta = -1$ or 4. The gain is less important because the systems are preconditioned. In conclusion, we can see that $\beta = -1$ stays good compromise for other types of geometries and for variable impedance operators. In what follows, we only use the parameter $\beta = -1$.

Table 3. Influence of the weight parameter β for two test cases.

Case	number of iterations $\beta = -1$	number of iterations $\beta = 4$
Object1-3	22	28
object3-2	17	21

6.2. A Comparison between the ICFIE1 and ICFIE2 in Term of Accuracy

In this section, we present a simple example which has motivated us to propose the ICFIE2 technique. For this purpose, we consider the object2. In this kind of problem ($\eta = 1$), we know that the BGLF is very accurate and consequently, it will be our reference method. Figure 2 shows the Radar Cross Section (RCS). The solution obtained by using the BGLF, ICFIE1 and ICFIE2 are very close except in the shaded region (see Figure 3). It is a zone which can be difficult to be restored correctly. One can clearly see the advantage to use the ICFIE2 in term of accuracy. In conclusion, the ICFIE2 could be needed to treat complex problems where an accurate solution is required.
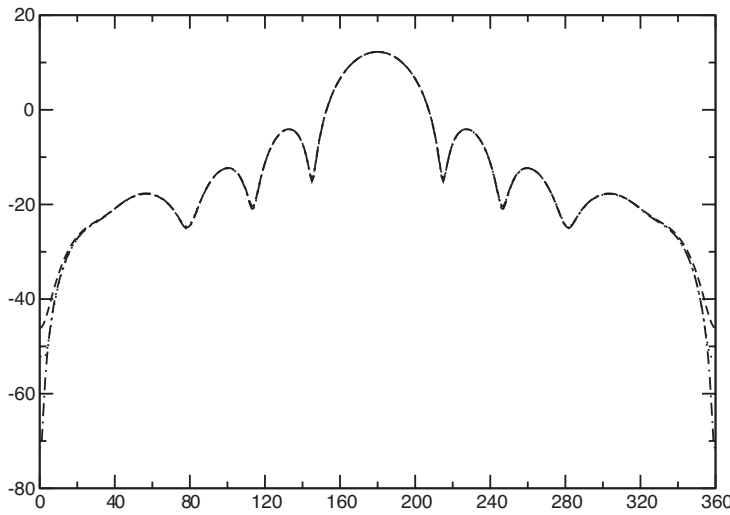

Figure 2. Comparison of the RCS of the cube obtained by different ICFIE algorithm for $\eta = 1$: $- \cdot$ BGLF, $\cdot\cdot$ ICFIE2, $- -$ ICFIE1.

6.3. Comparison with an Analytical Case

We consider the situations described by Object1-1 and Object1-2. The density of the preconditioner is identical for the formulations (BGLF and ICFIE) and is about 0.02%. Recall that we use the same preconditioner for the ICFIE1 and ICFIE2. The computing time of the preconditioner for the formulation ICFIE is about $9h$ and is more important than this obtained for the BGLF formulation ($5h$). It is due to the fact that we did not take into account that a part of the matrix
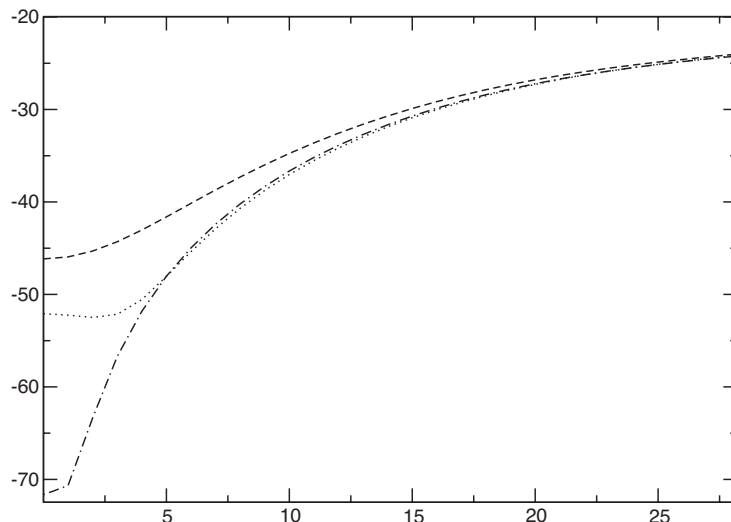
Figure 3. Zoom on the previous figure.

Table 4. Relative errors on the RCS for two values of η in the sphere case.

η	relative error on the RCS		
	BGLF	ICFIE1	ICFIE2
case 1	0.02%	0.4%	0.1%
case 2	0.02%	0.4%	0.1%

is sparse (see (29)); moreover, for the BGLF, the symmetry of the matrix has been used. Figure 4 gives the RCS for the three methods. It shows that the RCS are similar for the two cases. In the sphere case, the exact RCS can be computed using the Mie series. Table 4 contains the relative errors on the RCS. The three techniques give a numerical solution with a good accuracy. The relative error on the RCS is less than 0.5%. Moreover, we note that the ICFIE2 solution is slightly more accurate than the one of ICFIE1.

In order to compare the CPU time costs needed to obtain the solution, we have only considered the time coming from the matrix-vector products noted $t1$. Indeed, it represents the intrinsic cost of the method whereas the rest of the cost may be improved. More precisely, the BGLF CPU time directly is linked to $t1$ whereas for the ICFIE we take into account the FMM calculation, the inversion of the sparse matrices and communications between the processors. The time due
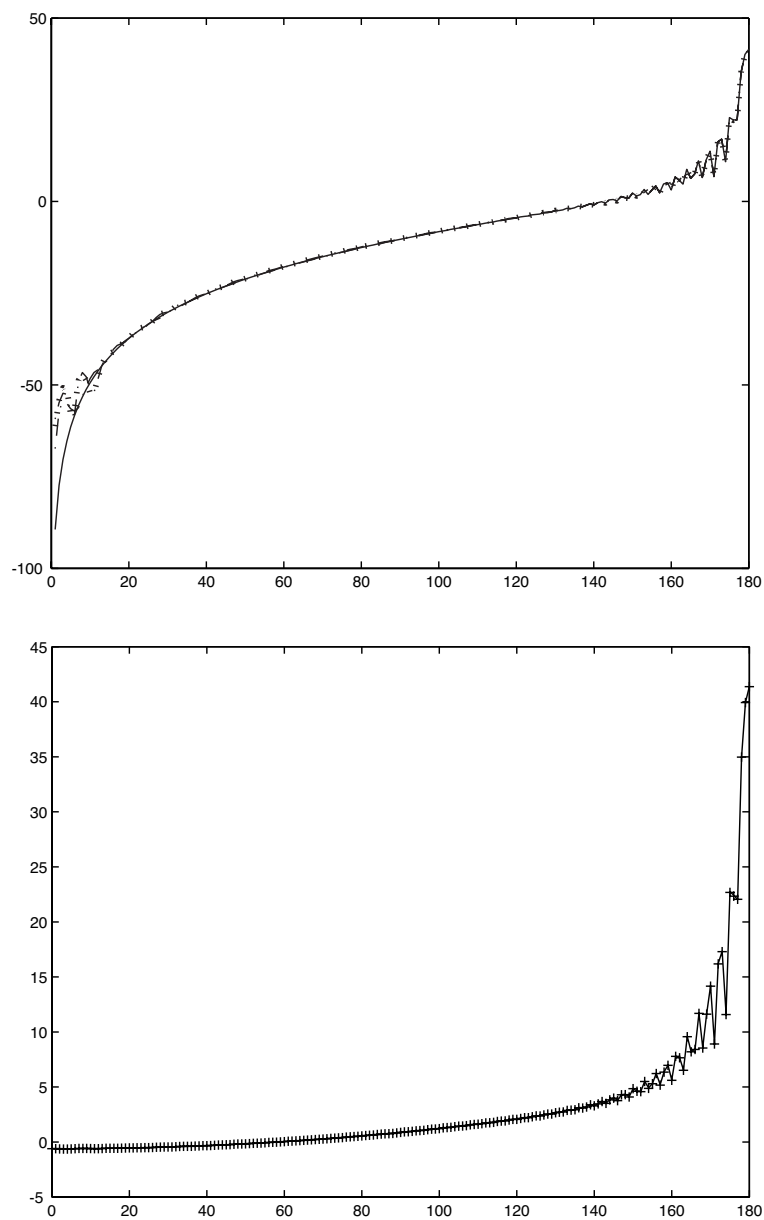
Figure 4. RCS of the sphere for the case 1 (up) and the case 2 (down) (–: Mie, –.: BGLF, –: ICFIE1, ..: ICFIE2).

to the vector product by the sparse matrices in the case of the ICFIE1 or ICFIE2 is noted by $t2$ and is also given. The CPU times $(t1, t2)$ and the iteration number n_{iter} are given in Table 5. The largest part of the time is taken by the FMM computation. With regard to the inversion of sparse matrices, ICFIE1 is better by a factor equal to about 10 in comparison with ICFE2. The time difference $t_1 - t_2$ for ICFIE1 is not the same as this obtained for the ICFIE2. It may be probably due to the communications between the processors. These latter are greater for the ICFIE2 method. For Object1-2, the CPU time for ICFIE1 and ICFIE2 is better by a factor about 4 in comparison with BGLF. Besides, for Object1-1, the performances are almost identical. Indeed, in this case, the BGLF system spectrum lies on a unique zone of the complex plane whereas for $\eta \neq 1$ it is scattered on two distinct zones. The phenomenon is due to the presence of the terms η and $1/\eta$ in the BGLF: these terms are the same when $\eta = 1$.

Table 5. Results obtained for the three methods in the sphere case.

	BGLF		ICFIE1		ICFIE2	
	case 1	case 2	case 1	case 2	case 1	case 2
n_{iter}	28	166	15	23	16	23
t1	$4h33$	$47h55$	$5h53$	$10h05$	$7h02$	$12h12$
t2	-	-	$130s$	$203s$	$1155s$	$1646s$

Table 6 contains the memory storage needed for the preconditioner and the close matrices. There is a factor equal to about 1.5 between the two methods in favor of BGLF.

Table 6. Memory storage needed for the preconditioner and the close matrices.

Memory (Gbytes)	BGLF	ICFIE
Preconditioner	12.484	3.1211
Close matrices	7.2802	26.776
Total	19.7642	29.8971

In conclusion, ICFIE1 and ICFIE2 are similar in terms of accuracy, robustness and CPU time spent for the case of the sphere with a constant impedance operator. Moreover, ICFIE is competitive for the two cases and is less expensive in time when the value of the impedance is different of 1.

6.4. Variable Value of Impedance

We consider the cases described by Object3. In particular, we want to study the effect of the impedance variation.

The density of the preconditioner is identical for the formulations (BGLF and ICFIE) and is about 0.07%. Again, as it is observed for the sphere case (see Section 6.3), the CPU time of the preconditioner for the formulation ICFIE is about $5h37$ and is greater about a factor 1.8 than this obtained for the BGLF formulation $(3h)$. Figure 5 shows the RCS for Case 1 and 2: all curves are very close. For the case 2, the BGLF solution has been obtained by using a flexible GMRES [20] which allows us to achieve the convergence. The CPU time needed to get the solution is about $241h$.

Note that the BGLF solution is taken as the reference solution. The accuracy results are summed up in Table 7. We can notice that the two solutions are similar in terms of RCS. One can also see a little increase of the error when the impedance becomes non constant.

Table 7. Relative error between the currents and the RCS in function of the value of the impedance operator.

Case	relative error on the currents		error on the RCS	
	ICFIE1	ICFIE2	ICFIE1	ICFIE2
case 1	4.8%	3.8%	0.9%	0.79%
case 2	11.7%	11.67%	2.06%	1.7%

Table 8 gives the number of iterations n_{iter} and the CPU times t_1 and t_2 needed for the construction of the solution. These times are defined in Section 6.3. One notices that:

- The number of iterations for the ICFIE does not depend very much on the value of the impedance. On the contrary, the BGLF is very sensitive to the variations of η and particularly when there is a perfectly conducting part on the surface of the obstacle.

- The important gain is obtained by using ICFIE1 or ICFIE2. Moreover, one can notice that it is directly connected to the gain in term of number of iterations.

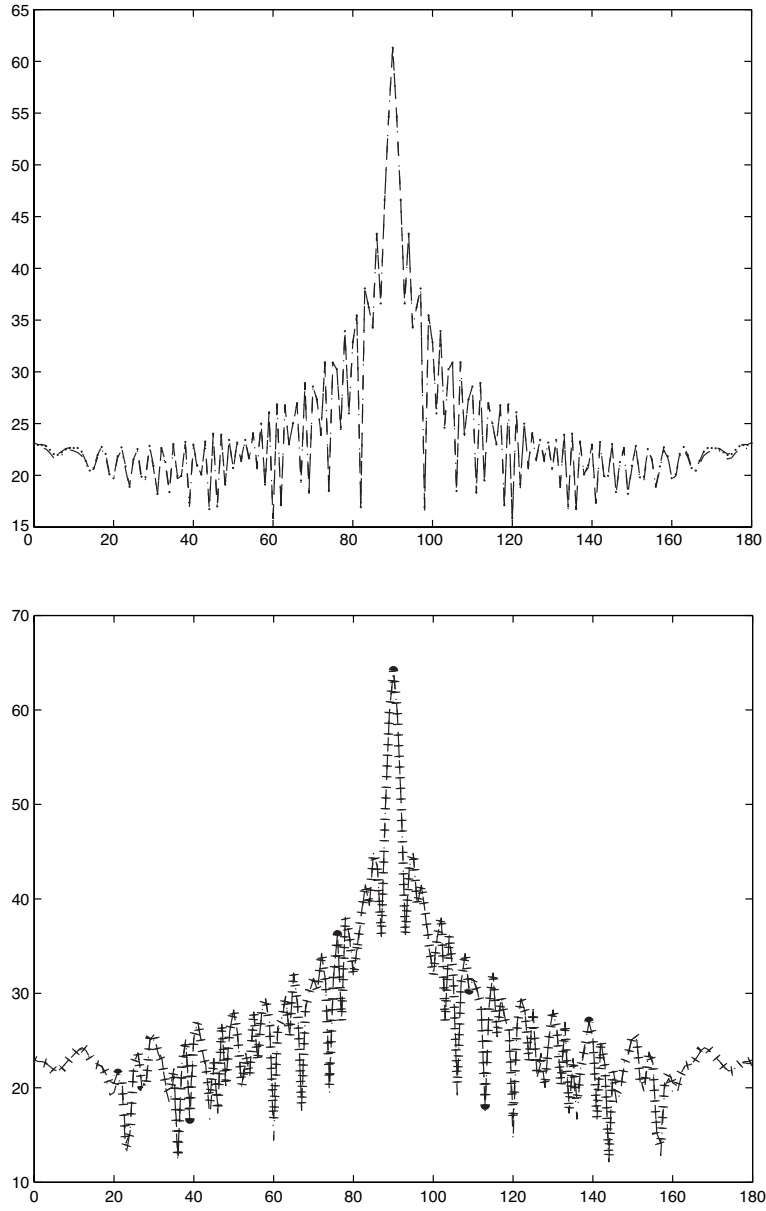In conclusion, the ICFIE is well appropriated to treat the partially coated objects.

Figure 5. RCS of the cylinder for the case 1 (up) and the case 2 (down) (–.: BGLF, –: ICFIE1, ..: ICFIE2).

Table 8. Results obtained in the cylinder case when the impedance value is variable.

	BGLF		ICFIE1		ICFIE2	
	case 1	case 2	case 1	case 2	case 1	case 2
n_{iter}	45	300	15	18	15	18
t1	$7h16$	$38h38$	$6h48$	$7h55$	$7h13$	$9h18$
t2	-	-	$144s$	$177s$	$1071s$	$1468s$

7. CONCLUSION

In this paper, we have studied a technique based on the CFIE formulation to solve electromagnetic scattering problems relative to an impedance boundary condition on an obstacle of arbitrary shape in the frequency domain. This formulation can be written with two terms, one which is directly linked to the CFIE term when the obstacle is perfectly conducting $A^{\beta}_{cfie}\mathbf{J}$ and another term which is related to $\mathbf{n} \times A^{\frac{1}{\beta}}_{cfie}\mathbf{M}$. This choice allows anyone who possesses a metallic CFIE solver to implement the ICFIE at lower cost. The magnetic current is computed via the impedance relation. Note that in the impedance relation, a $\mathbf{n}\times$ term appears. Two approaches have been proposed in order to treat correctly this term. We have proposed to eliminate the magnetic current and to keep only the electric current as unknown.

After discretization, the final system is solved with an iterative solver coupled with a FMM algorithm. We have proposed the construction of a SPAI preconditioner for this formulation.

The numerical results obtained show that ICFIE1 and ICFIE2 allow us to obtain accurate solutions which are close to BGLF's. Moreover, when the impedance value is small or variable, ICFIE algorithms converge faster and a CPU time gain is observed. In particular, we have shown that the ICFIE allows us to treat efficiently the partially coated objects. Finally, we get a more accurate solution for ICFIE2 in some cases.

REFERENCES

1. Leontovitch, M. A., "Approximate boundary conditions for the electromagnetic field on the surface of a good conductor," *Investigations Radiowave Propagation Part II*, Academy of Sciences, Moscow, 1978.

2. Monk, P., "Finite element methods for Maxwell's equations," *Numerical Mathematics and Scientific Computation*, Oxford Science Publication, 2003.

3. Stupfel, B., "A hybrid finite element and integral equation domain decomposition method for the solution of the 3-D scattering problem," *Journal of Computational Physics*, Vol. 172, No. 2, 451–471, September 20, 2001.

4. Collino, F., S. Ghanemi, and P. Joly, "Domain decomposition method for the Helmholtz equation: A general presentation," *Comput. Methods Appl. Mech. Eng.*, Vol. 184, Nos. 2–4, 171–211, 2000.

5. Boubendir, Y., "Techniques de décomposition de domaine et méthode d'équations intégrales," Ph.D. thesis, INSA, Juin 2002.

6. Rao, S. M., D. R. Wilton, and A. W. Glisson, "Electromagnetic scattering by surfaces of arbitrary shape," *IEEE Trans. Antennas Propagat.*, Vol. AP-30, 409–418, May 1982.

7. Bendali, A., M.'B. Fares, and J. Gay, "A boundary-element solution of the Leontovitch problem," *IEEE Transaction on Antennas and Propagation*, Vol. 47, No. 10, 1597–1605, 1999.

8. Ammari, H., C. Latiri-Grouz, and J. C. Nédélec, "Scattering of Maxwell's equations with a Leontovitch boundary condition in an inhomogeneous medium: A singular perturbation problem," *SIAM J. of Appl. Math.*, Vol. 59, 1322–1334, 1999.

9. Lange, V., "Equations intégrales espace-temps pour les équations de Maxwell. Calcul du champ diffracté par un obstacle dissipatif," Ph.D. thesis, Université de Bordeaux I, Oct. 1995.

10. Colton, D. and R. Kress, "Inverse acoustic and electromagnetic scattering theory," *Applied Mathematical Sciences*, Vol. 93, Springer, Berlin, 1992.

11. Rumsey, V. H., "Reaction concept in electromagnetic theory," *Physical Review*, Vol. 94, 1483–1491, 1954.

12. Makhlouf, A., "Résolution de problèmes de diffraction d'ondes électromagnétiques par équations intégrales de frontière avec condition d'impédance," CERFACS Working Note WN/EMC/04/93, 2004, available online: http://www.cerfacs.fr/emc/.

13. Nédélec, J. C., *Acoustic and Electromagnetic Equations Integral Representation for Harmonic Problems*, Springer, New-York, 2001.

14. Frayssé, V., L. Giraud, S. Gratton, and J. Langou, "A set of GMRES routines for real and complex arithmetics on high performance computers," CERFACS Technical Report, TR/PA/03/3,

available online: http://www.cerfacs.fr/algor/reports/algo_reports_2003.html.

15. Christiansen, S. H. and J.-C. Nédélec, "A preconditioner for the electric field integral equation based on Calderon formulas," *SIAM Journal on Numerical Analysis*, SINUM Vol. 40, Issue 3, 1100–1135, 2002.

16. Buffa, A. and S. H. Christiansen, "A dual finite element complex on the barycentric refinement," *Comptes Rendus Mathématique*, Vol. 340, Issue 6, 461–464, 2005.

17. Carpentieri, B., I. S. Duff, and L. Giraud, "A class of spectral two-level preconditioners," *SIAM J. Scientific Computing*, Vol. 25, No. 2, 749–765, 2003.

18. Hsiao, G. C. and R. E. Kleinman, "Mathematical foundations for error estimation in numerical solutions of integral equations in electromagnetics," *IEEE Transaction on Antennas and Propagation*, Vol. 45, No. 3, 316–328, 1997.

19. "Multifrontal massively parallel solver," available online: http://www.enseeiht.fr/lima/apo/MUMPS.

20. Frayssé, V., L. Giraud, and S. Gratton, "A set of flexible-GMRES routines for real and complex arithmetics," CER-FACS Technical Report, TR/PA/98/20, available online: http://www.cerfacs.fr/algor/reports/algo_reports_1998.html.

21. Brezzi, F. and M. Fortin, *Mixed and Hybrid Finite Element Methods*, Springer-Verlag, 1991.

22. Engquist, B. and J.-C. Nédélec, "Effective boundary conditions for acoustic and electro-magnetics scattering in thin layers," research report CMAP, Ecole Polytechnique, Palaiseau, France, 1993.

23. Chew, W.-C., J. Jin, E. Michielssen, and J. Song, *Fast and Efficient Algorithms in Computational Electromagnetics*, Artech House, 2001.

24. Collino, F. and F. Millot, "2-components algorithm for the multilevel fast multipole method for solving large scale diffraction problems," *JEE02 (European Symposium on Numerical Methods in Electromagnetics)*, Toulouse, France.

25. Collard, B., M'B. Fares, and B. Souny, "A new formulation for scattering by impedant 3D bodies," *J. of Electromagn. Waves and Appl.*, Vol. 20, No. 10, 1291–1298, 2006.

26. Jung, B. H., T. K. Sarkar, and Y.-S. Chung, "A survey of various frequency domain integral equations for the analysis of scattering form three-dimensional dielectric objects," *Progress In Electromagnetics Research*, PIER 36, 193–246, 2002.

27. Zhou, X., "On Helmoltz's theorem and its interpretations," *J. of Electromagn. Waves and Appl.*, Vol. 21, No. 4, 471–483, 2007.

28. Carpentieri, B., "Fast-iterative solution methods in electromagnetic scatteting," *Progress In Electromagnetics Research*, PIER 79, 151–178, 2008.

29. Bartoli and Bendali, "Robust and high-order effective boundary conditions for perfectly conducting scatterers," *IMA J. Appl. Math.*, Vol. 67, 479–508, 2002.

30. Wang, D.-S., "Limits and validity of the impedance boundary condition on penetrable surfaces," *IEEE Trans. Ant. Prop.*, Vol. 35, 453–457, October 1987.